The Sensitivity of the Proportionality between Temperature Change and Cumulative CO_2 Emissions to Ocean Mixing

Dana Ehlert and Kirsten Zickfeld

Simon Fraser University, Burnaby, British Columbia, Canada

Michael Eby

School of Earth and Ocean Sciences, University of Victoria, Victoria, and Simon Fraser University, Burnaby, British Columbia, Canada

Nathan Gillett

Canadian Centre for Climate Modelling and Analysis, Environment and Climate Change Canada, Victoria, British Columbia, Canada

(Manuscript received 29 March 2016, in final form 12 December 2016)

ABSTRACT

The ratio of global mean surface air temperature change to cumulative CO_2 emissions, referred to as transient climate response to cumulative CO_2 emissions (TCRE), has been shown to be approximately constant on centennial time scales. The mechanisms behind this constancy are not well understood, but previous studies suggest that compensating effects of ocean heat and carbon fluxes, which are governed by the same ocean mixing processes, could be one cause for this approximate constancy. This hypothesis is investigated by forcing different versions of the University of Victoria Earth System Climate Model, which differ in the ocean mixing parameterization, with an idealized scenario of 1% annually increasing atmospheric CO_2 until quadrupling of the preindustrial CO_2 concentration and constant concentration thereafter. The relationship between surface air warming and cumulative emissions remains close to linear, but the TCRE varies between model versions, spanning the range of 1.2°–2.1°C EgC^{-1} at the time of CO_2 doubling. For all model versions, the TCRE is not constant over time while atmospheric CO_2 concentrations increase. It is constant after atmospheric CO_2 stabilizes at 1120 ppm, because of compensating changes in temperature sensitivity (temperature change per unit radiative forcing) and cumulative airborne fraction. The TCRE remains approximately constant over time even if temperature sensitivity, determined by ocean heat flux, and cumulative airborne fraction, determined by ocean carbon flux, are taken from different model versions with different ocean mixing settings. This can partially be explained with temperature sensitivity and cumulative airborne fraction following similar trajectories, which suggests ocean heat and carbon fluxes scale approximately linearly with changes in vertical mixing.

1. Introduction

Recent literature has shown an approximately linear relationship between global warming and cumulative CO_2 emissions (Matthews et al. 2009; Allen et al. 2009; Eby et al. 2009). The ratio between global mean temperature change and cumulative emissions is referred to as transient climate response to cumulative CO_2 emissions (TCRE) but has also been called carbon–climate response (CCR) in earlier literature (e.g., Matthews et al. 2009). A useful application of the approximate constancy of the TCRE, especially for climate policy, is setting total allowable cumulative emissions to meet global warming targets (Zickfeld et al. 2009; Raupach et al. 2014). The Fifth Assessment Report of the Intergovernmental Panel on Climate Change gives a range for the TCRE of 0.8°–2.5°C $(1000\,PgC)^{-1}$ based on results from phase 5 of the Coupled Model Intercomparison Project (CMIP5) models and observational constraints (Collins et al.

Denotes content that is immediately available upon publication as open access.

Supplemental information related to this paper is available at the Journals Online website: http://dx.doi.org/10.1175/JCLI-D-16-0247.s1.

Corresponding author e-mail: Dana Ehlert, dehlert@sfu.ca

DOI: 10.1175/JCLI-D-16-0247.1

2013; Frölicher and Paynter 2015). The TCRE differs between models as it includes both the physical and biogeochemical uncertainties of the models, which makes it a useful benchmark for model intercomparison (Collins et al. 2013; Bindoff et al. 2013).

For any one specific model the TCRE is approximately constant over time and across CO_2 emissions with certain limitations to that constancy for different models. The limits of this approximate constancy have been studied in terms of cumulative CO_2 emissions and emission rates. Earlier studies suggest strongest divergence from a constant value occurs under very low cumulative emissions (<1000 PgC) because the signal-to-noise ratio is too low (Gillett et al. 2013) and very high cumulative emissions (>3000 PgC) because the effect of saturating radiative forcing is stronger than the saturation of carbon sinks (Gillett et al. 2013; Herrington and Zickfeld 2014). However, a recent study suggests that a large decrease in the TCRE for high cumulative emissions is only associated with some models of intermediate complexity, and the TCRE remains close to constant for most models [including the University of Victoria (UVic) Earth System Climate Model (ESCM)] for cumulative emissions of up to 5000 PgC (Tokarska et al. 2016). The TCRE is also not constant for stabilization of the climate system over several thousand years (Collins et al. 2013; Frölicher and Paynter 2015). In some models the TCRE is also not constant under very high emissions rates, like an instantaneous quadrupling of preindustrial atmospheric CO_2 concentrations (Gillett et al. 2013). Additionally, the TCRE may vary to second order for some models with emission rate. Krasting et al. (2014) find that the TCRE is highest for low and high emission rates (2 and 25 PgC yr^{-1}) but is lower for current emission rates (5–10 PgC yr^{-1}), while Herrington and Zickfeld (2014) find a decrease in TCRE with increasing emissions rates. Thus the TCRE may be scenario dependent in some climate models, but these variations are smaller than intermodel variation in the TCRE (Krasting et al. 2014; Herrington and Zickfeld 2014; Leduc et al. 2015). Zickfeld et al. (2016) show that the TCRE is not constant when positive CO_2 emissions are followed by net-negative CO_2 emissions because of the lagged response of the deep ocean.

The physical explanation for the approximate constancy of the TCRE remains under discussion and different explanations have been proposed. Matthews et al. (2009) separate the TCRE into airborne fraction of cumulative CO_2 emissions (change in atmospheric carbon burden per unit change in cumulative emissions) and temperature change per unit change in atmospheric carbon burden. Using these two ratios, Matthews et al. (2009) explain the constancy TCRE with two cancellation processes: First, the approximate constancy of the TCRE across scenarios is due to the cancellation of an increase in the airborne fraction of cumulative emissions with increase in emission rate, which means more warming, and a saturation of radiative forcing from CO_2 with increasing atmospheric CO_2, which means less warming. The cumulative airborne fraction increases at higher emissions because the carbon uptake rate by land and ocean decreases. Second, the approximate temporal constancy of the TCRE is due to the cancellation of a decrease in airborne fraction of cumulative emissions over time (i.e., less warming) and an increase in temperature change per unit change in atmospheric CO_2, meaning more warming. Matthews et al. (2009) and Solomon et al. (2009) suggest that the second cancellation process could be due to ocean heat and carbon fluxes being determined by the same deep ocean mixing processes. Goodwin et al. (2015) show a cancellation over time of the sensitivity of surface warming to radiative forcing and the sensitivity of radiative forcing to cumulative emissions due to compensating effects of ocean heat and carbon fluxes on the climate. The sensitivity of surface warming to radiative forcing increases over time as a result of decreasing ocean heat uptake per unit radiative forcing (i.e., more warming). At the same time, the sensitivity of radiative forcing to cumulative emissions decreases over time because the radiative forcing is directly proportional to undersaturated oceanic carbon, and oceanic carbon content gets closer to equilibrium with the atmospheric carbon content. It should be noted that Goodwin et al. (2015) focus their discussion on the time after emissions are set to zero, when the climate system is not externally forced anymore and approaches equilibrium (i.e., ocean heat and carbon fluxes are declining). Another study by Williams et al. (2016) expands the Goodwin et al. (2015) approach to simulations that include non-CO_2 forcers along with CO_2 forcing. Williams et al. (2016) find close to constant but slightly increasing TCRE for two Earth system models on long time scales. On decadal time scales they find strong temporal variations in the TCRE resulting from non-CO_2 forcers.

MacDougall and Friedlingstein (2015) suggest that for constant CO_2 emission rates, the cumulative airborne fraction is approximately constant over time and that the constancy of the TCRE is due to the cancellation within the physical response of the climate system. They argue that the decline in ocean heat flux rate over time and diminished radiative forcing per unit atmospheric CO_2 increase have opposite effects on temperature and cancel each other out. A constant cumulative airborne fraction does not seem plausible as this would imply a constant temperature change per unit change in

atmospheric CO_2, which has been shown to not be the case (Gregory et al. 2015). Other studies using the same climate model further showed an increase in cumulative airborne fraction over time, especially for higher constant emission rates (Herrington and Zickfeld 2014; Leduc et al. 2015). For exponentially increasing CO_2 emission rates over time, MacDougall and Friedlingstein (2015) suggest that while emission rates increase the ocean heat uptake rate increases, which has a cooling effect, and the ocean carbon uptake fraction (change in ocean carbon per cumulative emissions) declines, which leads to a higher cumulative airborne fraction of CO_2 and thus higher radiative forcing and more warming. They conclude that their finding supports the hypothesis of the TCRE being constant as a result of ocean heat and carbon fluxes being governed by the same process of deep ocean mixing. However, the role of ocean heat flux in the constancy of the TCRE is not addressed in depth.

The commonly given hypothesis of the same mechanism governing ocean heat and carbon fluxes causing an approximately constant TCRE can be questioned as there are important differences in the location and magnitude of ocean heat and carbon fluxes and the processes by which they are affected. For example, under a warming climate, changes in ocean circulation affect ocean heat storage more strongly than ocean carbon storage because changes in ocean circulation shift ocean heat uptake to higher latitudes, which increases the cooling effect of the heat flux. Global redistribution of ocean carbon, on the other hand, has no effect on ocean carbon uptake (Winton et al. 2013). This is partially due to the different boundary conditions for ocean heat and carbon uptake; atmospheric surface temperature has a strong meridional gradient whereas atmospheric CO_2 is equally distributed over the globe. Furthermore, only ocean carbon flux is directly affected by marine biology and carbonate chemistry. Additionally, the sea–air equilibration time scale is around nine months for carbon but only less than a month for heat (Frölicher et al. 2015).

To gain further understanding of the physical and biogeochemical processes determining the constancy of the TCRE, the effect of ocean mixing parameterization on ocean heat and carbon fluxes and, in turn, on the TCRE is explored in this study. Ocean mixing from small-scale circulation processes, which cannot be resolved in climate models, must be parameterized. Changing this ocean mixing parameterization will affect how tracers, such as heat and carbon, are distributed within the ocean and at the ocean surface, which in turn affects ocean heat and carbon uptake. This study will also explore the sensitivity of the TCRE to ocean mixing, which may be helpful in explaining the differences in the TCRE between models.

Section 2a describes the model used, section 2b introduces the performed simulations, and section 2c explains the analytic framework applied to the simulation results. The results of the model simulations are presented in section 3, including a discussion of the effect of ocean mixing on ocean heat and carbon fluxes, differences in the TCRE between mixing settings, and the temporal evolution of the TCRE. Section 4 presents our conclusions.

2. Methods

a. Model description

For this study the University of Victoria (UVic) Earth System Climate Model, version 2.9 (ESCM 2.9), was used. It consists of the following coupled components: a fully dynamic ocean circulation model, an energy–moisture balance atmosphere model, a dynamic–thermodynamic sea ice model, and a land surface and terrestrial vegetation model. It also includes land, ocean, and ocean sediment carbon cycle components. All components have a resolution of 1.8° (meridional) × 3.6° (zonal). Because of the simple atmosphere, this model is considered to be an Earth system model of intermediate complexity (Eby et al. 2009).

The atmosphere is represented by a vertically integrated energy–moisture balance model. It includes water vapor feedback, planetary longwave radiative feedback, and dynamic wind feedbacks but no cloud feedbacks. Clouds are however represented in the atmosphere's albedo.

The land is modeled via a simplified version of the land surface scheme Met Office Surface Exchange Scheme (MOSES) (Meissner et al. 2003; Cox et al. 1999), which is coupled to the dynamic vegetation model Top-down Representation of Interactive Foliage and Flora Including Dynamics (TRIFFID) (Cox 2001). The ocean is represented via the Geophysical Fluid Dynamics Laboratory (GFDL) Modular Ocean Model, version 2.2 (MOMv2.2), which is a 3D general circulation model. It consists of 19 layers with variable thickness, ranging from 50 m at the top to 518 m at the bottom, and a total depth of 5396 m (Weaver et al. 2001). The ocean model is coupled to a dynamic–thermodynamic sea ice model, wherein sea ice is affected by ocean dynamics, atmospheric wind fields, and phase transitions (Weaver et al. 2001). Furthermore, the ocean module includes inorganic and organic carbon cycle components. The inorganic carbon component mainly describes the change in inorganic ocean carbon

TABLE 1. Description of different model versions and their names as referred to in the text and figures. The term A_h is the diffusivity along isopycnals, A_{thkdff} is the eddy thickness diffusivity as introduced by Gent and McWilliams (1990), and k_v is the vertical diffusivity. Preindustrial state of the different model versions shown are exemplarily for the following variables: global mean surface air temperature (SAT), MOC ($1\,\text{Sv} \equiv 10^6\,\text{m}^3\,\text{s}^{-1}$; the given values refer to the maximum of the streamfunction), and total ocean carbon storage C_O.

Experiment	A_h ($\text{m}^2\,\text{s}^{-1}$)	A_{thkdff} ($\text{m}^2\,\text{s}^{-1}$)	Vertical mixing scheme	k_v ($\text{cm}^2\,\text{s}^{-1}$)	SAT (°C)	MOC (Sv)	C_O (PgC)
Default	800	800	Bryan–Lewis	0.3–1.3	13.39	21.6	37 297
$k_{v,\text{const}}$ 0.05	800	800	Vertically constant	0.05	12.89	9.8	37 910
$k_{v,\text{const}}$ 0.3	800	800	Vertically constant	0.3	13.33	21.4	37 386
$k_{v,\text{const}}$ 1.0	800	800	Vertically constant	1.0	16.67	32.3	36 229
$k_{v,\text{B\&L}}$ low	800	800	Bryan–Lewis	0.1–1.1	13.16	12.7	37 919
$k_{v,\text{B\&L}}$ high	800	800	Bryan–Lewis	0.5–1.5	13.52	25.8	36 820
$k_{v,\text{tidal}}$ 0.1	800	800	Tidal	0.1	13.15	14.4	37 753
$k_{v,\text{tidal}}$ 0.2	800	800	Tidal	0.2	13.32	19.3	37 511
$k_{v,\text{tidal}}$ 0.45	800	800	Tidal	0.45	13.49	25.8	36 854
A_h 2400	2400	800	Bryan–Lewis	0.3–1.3	13.44	20.2	37 300
A_{thkdff} 400	800	400	Bryan–Lewis	0.3–1.3	13.44	23.9	37 120
$A_h A_{\text{thkdff}}$ 1600	1600	1600	Bryan–Lewis	0.3–1.3	13.35	16.6	37 596

from sea–air carbon flux and precipitation/evaporation, transport, and seawater carbon chemistry (Ewen et al. 2004). The organic cycling of carbon is modeled via a marine ecosystem model that includes nutrient supply, phytoplankton, zooplankton, and detritus (NPZD) (Schmittner et al. 2005). Sediment processes are represented using an oxic-only model of sediment respiration (Archer 1996).

Ocean mixing is described via momentum diffusivity (or viscosity) and tracer diffusivity (Weaver et al. 2001). In the following, ocean mixing always refers to the mixing of tracers. This tracer mixing can be described either in horizontal (vertical) or isopycnal (along surface of constant density) (diapycnal) direction. Either a horizontal- or an isopycnal-mixing scheme can be used, which accounts for diffusion along isopycnals, also referred to as Redi diffusion. A parameterization for mesoscale eddies, Gent–McWilliams thickness diffusion (Gent and McWilliams 1990; Weaver et al. 2001), can be added to the isopycnal-mixing scheme. The Gent–McWilliams thickness diffusivity accounts for mixing resulting from baroclinic instability in areas where isopycnals are tilted.

Because of isopycnal slope limitations in the ocean model, there is no practical difference between vertical and diapycnal mixing, and so a vertical mixing scheme is always applied. The vertical tracer diffusivity can be described with three different schemes: 1) vertically and laterally constant, 2) increasing with depth but laterally constant (Bryan–Lewis parameterization; Weaver et al. 2001), and 3) tidal mixing scheme, where mixing resulting from the dissipation of tidal energy at topography is added to the constant background diffusion parameter (Schmittner et al. 2005). The default option in the model is isopycnal mixing with the Gent–McWilliams parameterization (diffusivities of $800\,\text{m}^2\,\text{s}^{-1}$) for mesoscale eddies and Bryan–Lewis scheme for the vertical tracer diffusivity (diffusivity of $0.3\text{–}1.3\,\text{cm}^2\,\text{s}^{-1}$) (Weaver et al. 2001).

b. Experiment design

Different model versions were generated by changing the ocean mixing parameterization for tracer mixing (Table 1). The ocean mixing parameters are chosen to achieve an alteration of the ocean fluxes that is as large as possible while keeping the model stable and not necessarily to use parameters that closely reproduce observed ocean tracer distributions. However, to ensure the model does not transition into a different ocean circulation state we monitored the location of deep-water formation. The default vertical mixing scheme in the UVic ESCM is the Bryan–Lewis parameterization, which has lower vertical diffusivity k_v in the upper ocean and higher vertical diffusivity in the deeper ocean. When moving to higher or lower parameter values, the shape of the curve of k_v over depth was maintained but the curve was shifted to higher or lower values by changing the values of the vertical mixing parameter k_v as shown in Table 1. Values were set to a range between 0.1 (upper ocean) and $1.5\,\text{cm}^2\,\text{s}^{-1}$ (deep ocean), but the difference between lower and upper value of k_v was maintained. Different model versions were created by changing to a vertically constant mixing parameter and varying this parameter between 0.05 and $1.0\,\text{cm}^2\,\text{s}^{-1}$ or by using the tidal mixing scheme (Schmittner et al. 2005) in which the background diffusion parameter $k_{v,\text{tidal}}$ was changed. The values for the background diffusivity in the tidal mixing scheme were chosen based on Schmittner et al. (2009), Goes et al. (2010), and Ross et al. (2012) with a range between 0.1 and $0.45\,\text{cm}^2\,\text{s}^{-1}$. Mixing along isopycnals was also varied. The parameter for diffusion along isopycnals and eddy thickness diffusion were changed individually and together between

400 and 2400 $m^2 s^{-1}$. Traditionally, parameters for both mixing types were set to the same value. However, recent studies suggest that the diffusion along isopycnals might be higher (as seen in measurements) than the eddy thickness diffusion (Gnanadesikan et al. 2015a). Both lower eddy thickness diffusion and the same values for both parameters are used in this study.

All model versions are spun up for 6000 yr with prescribed constant atmospheric CO_2 concentration at preindustrial levels. Initialized from this preindustrial equilibrium state, all model versions are forced with a yearly 1% increase in atmospheric CO_2 levels up to a quadrupling of the preindustrial atmospheric CO_2 concentration (simulation years 0–139), followed by constant atmospheric CO_2 concentration (simulation years 140–1200). All other anthropogenic and natural forcings were held constant at preindustrial levels. As atmospheric CO_2 levels were prescribed, CO_2 emissions were diagnosed from the rate of increase in atmospheric CO_2 and land and ocean carbon fluxes.

For a comparison of the different climate states between the model versions the preindustrial global mean surface air temperature (SAT), maximum meridional overturning circulation (MOC), and ocean carbon storage are given in Table 1. In the following all comparisons are made to the values for the default mixing setting. Strongest changes occur under changes in vertical mixing parameter but not mixing scheme. Increased vertical mixing leads to a higher global mean SAT, stronger MOC, and lower ocean carbon storage. A stronger MOC leads to less sea ice and a lower surface albedo, which in turn leads to higher temperatures. Increased mixing along isopycnals leads to negligible change in ocean carbon storage, global mean SAT, and MOC. Lower eddy thickness diffusivity leads to negligible changes in global mean SAT, slightly decreased ocean carbon storage, and a slightly increased MOC. When both mixing along isopycnals and eddy thickness diffusivity are increased, global mean SAT does not change but MOC and ocean carbon storage increase. The effects of changes in ocean mixing on the MOC are discussed in detail by Schmittner and Weaver (2001). Though they used a different model, we observe similar effects of changes in mixing on the MOC. At the end of the spinup the global distribution of ocean heat uptake is similar between model versions, but the global distribution of ocean carbon uptake differs slightly (see Figs. S1 and S2 in the supplementary material). For low vertical mixing, irrespective of the mixing scheme, carbon uptake into the ocean increases relative to the model version with default mixing setting in the southern Pacific and Atlantic along a band between the southern tip of Africa, South America, and Australia. But parallel to this band is also an increase of carbon flux into the atmosphere from the ocean. Outgassing of carbon decreases in the equatorial Pacific with decreasing vertical mixing. Outgassing increases in the Southern Ocean, south of Australia, under increased isopycnal diffusivity.

c. *Theoretical framework for the TCRE*

To investigate which variables affect the TCRE and how these variables differ between model versions we write the TCRE as follows:

$$\mathrm{TCRE} = \frac{\Delta T}{\mathrm{CE}} = \frac{\Delta C_A}{\mathrm{CE}} \frac{\mathrm{RF}}{\Delta C_A} \frac{\Delta T}{\mathrm{RF}}, \tag{1}$$

where ΔC_A is the change in atmospheric carbon in petagrams of carbon (PgC), CE are the cumulative CO_2 emissions in PgC, RF is the radiative forcing in watts per square meter, and ΔT is the change in global mean surface air temperature in degrees Celsius.

The airborne fraction of cumulative emissions $\Delta C_A/\mathrm{CE}$ can be rewritten as a function of the ocean carbon uptake fraction $\Delta C_O/\mathrm{CE}$ and land carbon uptake fraction $\Delta C_L/\mathrm{CE}$ using the carbon budget equation $\mathrm{CE} = \Delta C_A + \Delta C_O + \Delta C_L$, where ΔC_O and ΔC_L are the change in ocean and land carbon reservoirs:

$$\frac{\Delta C_A}{\mathrm{CE}} = 1 - \left(\frac{\Delta C_O}{\mathrm{CE}} + \frac{\Delta C_L}{\mathrm{CE}} \right). \tag{2}$$

Using an energy balance equation for global mean temperature change,

$$\Delta T = \frac{1}{\lambda} \left(1 - \frac{N}{\mathrm{RF}} \right) \mathrm{RF}, \tag{3}$$

where λ is the feedback parameter in watts per square meter per degree Celsius and N is the net heat flux into the climate system in watts per square meter, the TCRE can be expressed as follows:

$$\mathrm{TCRE} = \left(1 - \frac{\Delta C_O + \Delta C_L}{\mathrm{CE}} \right) \frac{\mathrm{RF}}{\Delta C_A} \frac{1}{\lambda} \left(1 - \frac{N}{\mathrm{RF}} \right). \tag{4}$$

The first term in Eq. (4) is the cumulative airborne fraction (i.e., the fraction of cumulative CO_2 emissions that remains in the atmosphere and is not taken up by land and ocean sinks). The second term, $\mathrm{RF}/\Delta C_A$, is the radiative forcing sensitivity to an increase in CO_2 in the atmosphere. The last term of Eq. (4), $\lambda^{-1}[(1 - (N/\mathrm{RF})]$, is the temperature sensitivity. If the radiative forcing is taken at the time of doubling of the preindustrial atmospheric CO_2, this term multiplied with the radiative forcing is the transient climate response (TCR). The TCR describes the physical response of the climate

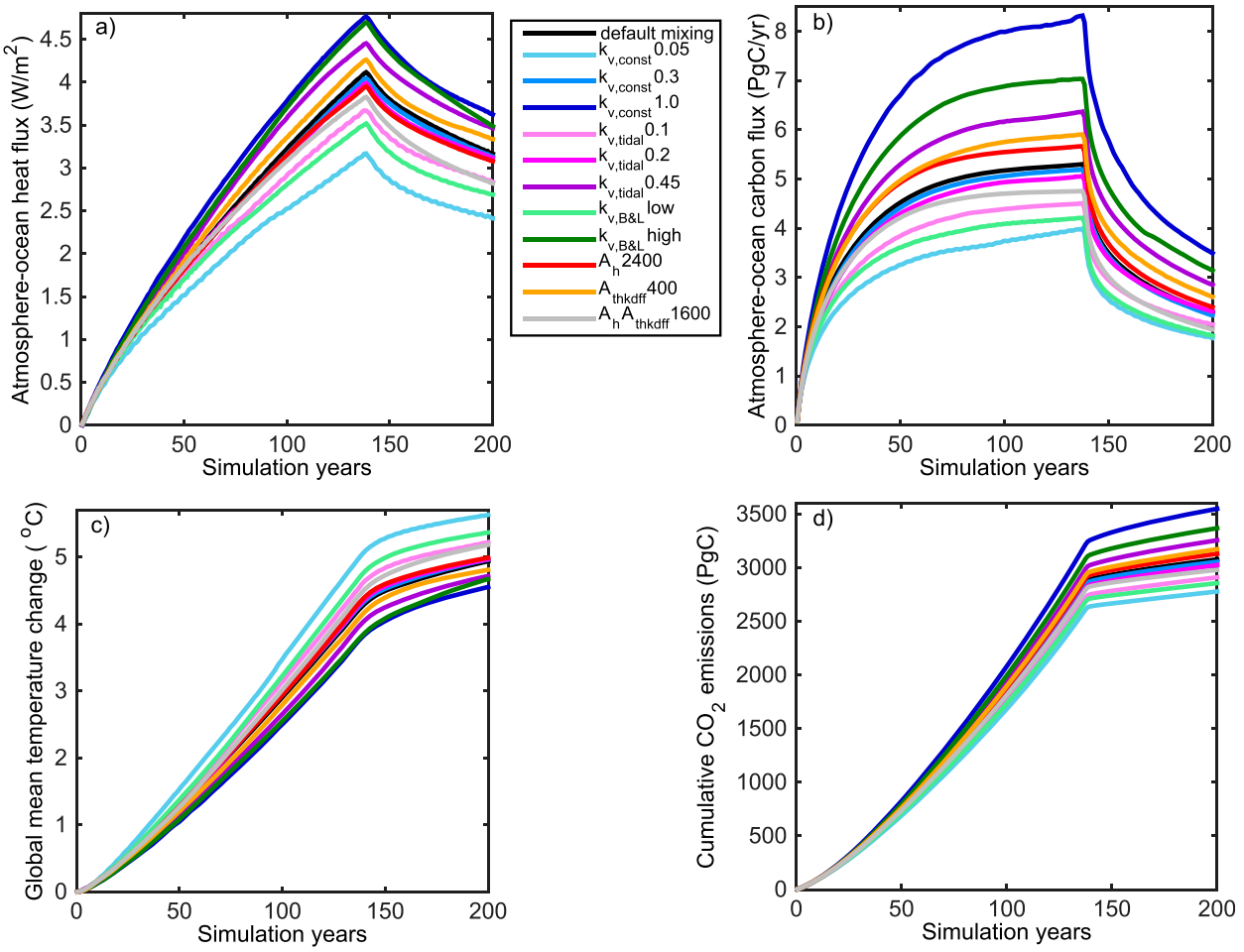

FIG. 1. Global mean (a) ocean heat and (b) carbon fluxes for the model versions with different mixing settings, under increasing atmospheric CO_2 levels (years 0–139) and 50 yr of constant atmospheric CO_2. Positive fluxes indicate uptake of heat or carbon by the ocean (i.e., a flux from the atmosphere into the ocean). Global mean (c) surface air temperature change relative to year 0 and (d) cumulative CO_2 emissions for the different model versions, under increasing atmospheric CO_2 levels (years 0–139) and 50 yr of constant atmospheric CO_2. Model versions with higher ocean heat and carbon fluxes have lower warming and stronger increases in cumulative emissions. Changes in vertical mixing (blue and green curves) have a stronger effect on temperature change and cumulative emissions than changes in mixing along isopycnals (yellow and red curves) compared to the default setting (black curve).

system to CO_2 forcing and is a useful metric to compare the physical response of different climate models. Equation (4) shows the effect of ocean heat and carbon uptake on the TCRE. The TCRE depends directly on ocean heat uptake, but it also depends on the change in the land and ocean carbon reservoirs (i.e., the integrals of the carbon fluxes in and out of these reservoirs).

3. Results and discussion

a. *Effect of ocean mixing on ocean heat and carbon fluxes in forced simulations*

Forcing the different model versions with increasing atmospheric CO_2 levels results in different heat and carbon fluxes between the model versions (Figs. 1a,b). In all simulations, globally averaged ocean heat and carbon uptake increase while atmospheric CO_2 levels rise and decrease after atmospheric CO_2 is stabilized. Increased vertical mixing leads to an increase in ocean heat and carbon uptake as higher vertical mixing increases the rate of mixing between the mixed layer and the deeper ocean (cf. highest and lowest vertical diffusion parameter for each mixing scheme; i.e., dark blue, dark purple, and green curves to light blue, light purple, and light green curves in Figs. 1a,b). Deep ocean water is cold and less equilibrated with increasing atmospheric CO_2 levels, and thus heat and carbon uptake increase. Increased ocean heat and carbon uptake and a less stratified ocean due to increased vertical mixing have also been shown in other studies (Goes et al. 2010; Olson et al. 2012; Schmittner

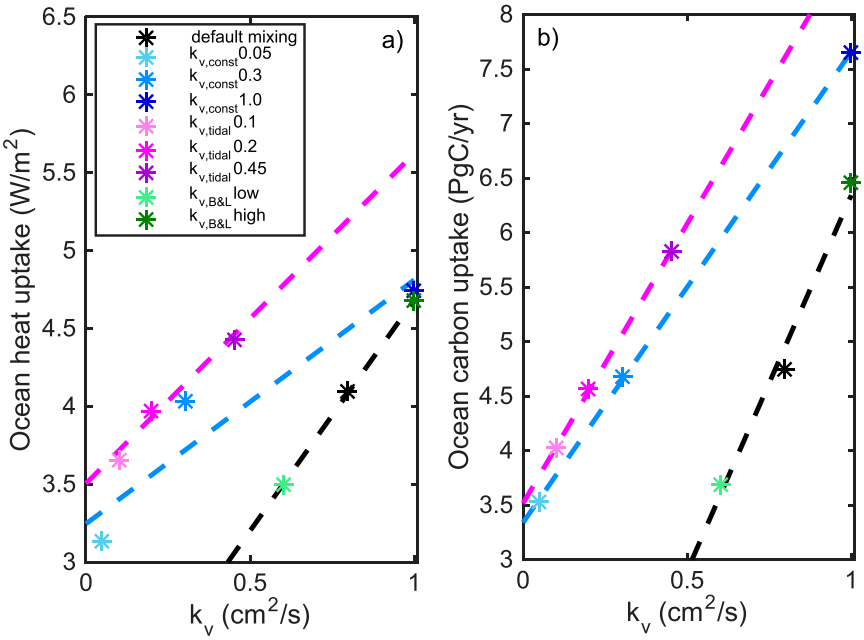

FIG. 2. (a) Ocean heat and (b) carbon uptake at year 140 as function of vertical mixing parameter k_v. The black, blue, and pink lines are the linear correlations (ordinary least squares regression) between the ocean uptake and the mixing parameter for the Bryan–Lewis, vertically constant, and tidal mixing schemes, respectively. The r^2 values are 0.99 ($p \leq 0.09$) for all correlations except for the correlation of constant vertical mixing and ocean heat uptake, where r^2 is 0.91 ($p = 0.13$). Therefore, the correlations are strong and significant, except in the latter case.

et al. 2009). However, these studies only used the tidal mixing scheme. If CO_2 emissions are prescribed and atmospheric CO_2 can evolve freely, increased ocean heat and carbon uptake as a result of increased vertical mixing have been shown to contribute equally to reduced warming (Schmittner et al. 2009). Correspondingly, decreased vertical mixing results in decreased ocean heat and carbon uptake. Interestingly, ocean heat and carbon uptakes correlate linearly with the vertical mixing parameter within each mixing setting (Fig. 2).

Lower eddy thickness diffusivity leads to increased overturning circulation (Gnanadesikan 1999), which leads to slightly increased ocean heat and carbon uptake compared to the default setting (cf. yellow curve vs black curve in Figs. 1a,b). Increased diffusivity along isopycnals leads to the smallest difference in heat and carbon uptake relative to the default setting compared to changes in the other mixing parameters, even though the relative changes in the diffusion parameter compared to the default setting are the strongest for the parameter of diffusion along isopycnals. A slightly higher increase in ocean carbon flux and slightly lower increase in ocean heat flux compared to the default setting can be observed (cf. red curve vs black curve in Figs. 1a,b). Changes in ocean heat and carbon uptake, relative to the uptake in the default mixing setting, are opposite in sign, and the change in ocean carbon flux is stronger in magnitude than the change in ocean heat flux. One possible explanation for lower ocean heat uptake compared to the default setting under increased atmospheric CO_2 is that increased mixing along isopycnals leads to a warmer surface ocean at higher latitudes, which in some areas leads to an increase in ocean heat loss, especially in the North Atlantic. A meridional redistribution of temperature in the surface ocean affects ocean heat flux, but a redistribution of carbon does not affect ocean carbon flux because atmospheric temperature has a meridional gradient and atmospheric carbon is globally equally distributed. An explanation for the slight increase in ocean carbon uptake could be changes in marine biology. Simulations with increased isopycnal diffusivity show less carbon outgassing and increased net primary productivity rates in the upwelling regions of the east equatorial Pacific, as more nutrients are available at the surface. Thus, the increase in globally averaged ocean carbon uptake could be explained with changes in ocean biology, which only affects ocean carbon but not ocean heat uptake. Increased ocean carbon uptake under increased diffusivity along isopycnals, partially

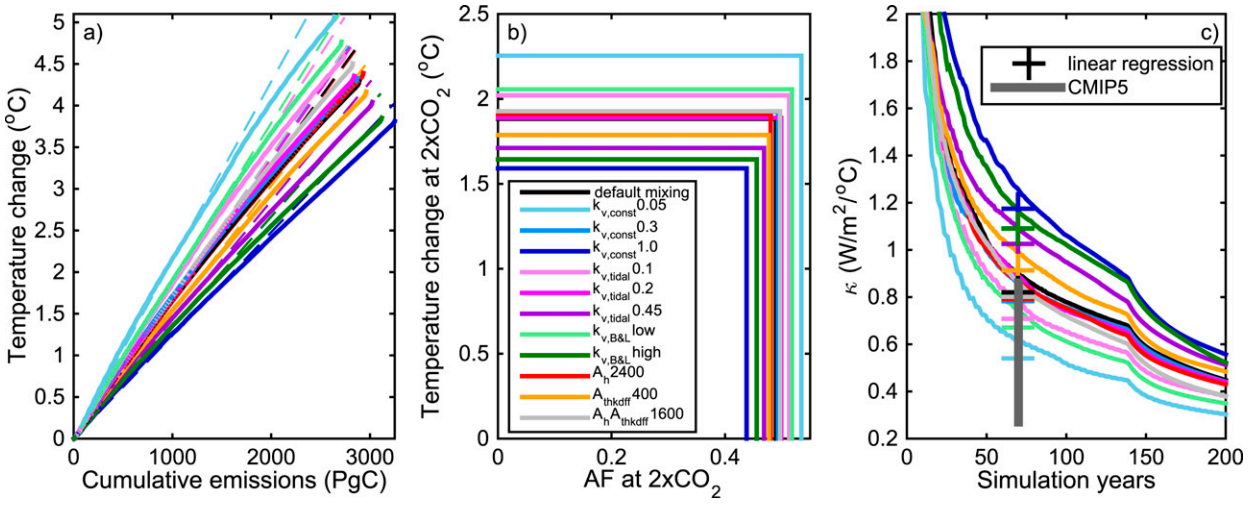

FIG. 3. (a) Global mean surface air temperature change (as shown in Fig. 1c) vs cumulative CO_2 emissions over the time period of increasing CO_2 concentration (simulation years 0–139). The slope of the curves is the TCRE, with a steeper slope indicating a higher TCRE value. The dashed lines are hypothetically constant TCRE values, using the TCRE value at the time of doubling atmospheric CO_2 levels. (b) Temperature change (relative to simulation year 0) at time of doubling of CO_2, referred to as TCR, vs the airborne fraction of cumulative CO_2 emissions (AF) at the time of CO_2 doubling for different model versions. (c) Ocean heat uptake efficiency κ, defined as ratio of net heat flux into the climate system (note that the latter is different from the ocean heat flux shown in Fig. 1, which is averaged over the surface area of the ocean rather than the entire Earth surface) to global mean surface air temperature change, over time. The efficiency is only shown for 60 yr after quadrupling of atmospheric CO_2 is reached for readability reasons, but the efficiency continues to decline for all model versions under constant atmospheric CO_2. The gray bar indicates the CMIP5 ocean heat uptake efficiency range (Kuhlbrodt and Gregory 2012), and the crosses indicate the ocean heat uptake efficiency, both calculated via an ordinary least squares regression between net heat flux into the climate system and global mean surface air temperature change over the first 70 simulation years.

due to increased biological carbon storage, has also been found in another study using a complex Earth system model (Gnanadesikan et al. 2015b).

Increasing both mixing along isopycnals and eddy thickness diffusivity (simulation "$A_h A_{\mathrm{thkdff}}$ 1600") leads to a decline in both ocean heat and carbon uptake. Assuming that changes in ocean heat and carbon uptake resulting from variations in the eddy thickness diffusivity are symmetric, increased eddy thickness diffusivity would lead to decreased ocean heat and carbon uptake, but an increased diffusion parameter along isopycnals leads to lower ocean heat uptake and higher ocean carbon uptake. The changes in ocean heat and carbon uptake in $A_h A_{\mathrm{thkdff}}$ 1600 show that changes in the eddy thickness diffusivity outweigh changes in the diffusion parameter along isopycnals. This result agrees with another study (Gnanadesikan et al. 2015b).

Our results suggest that changes in eddy thickness diffusivity, vertical mixing parameter, and/or vertical mixing scheme scale ocean heat and carbon uptake up or down but do not significantly affect the temporal evolution of the uptake.

b. *Effect of different mixing settings on the TCRE*

Differences in ocean heat and carbon uptake lead to different TCRE values between model versions. Higher ocean heat uptake leads to less surface air warming because more heat is taken up by the ocean. This can also be seen in Eq. (3). Higher ocean carbon uptake leads to higher cumulative emissions because if more carbon is taken up by the ocean, more carbon can be emitted in order to reach the same atmospheric CO_2 level.

For both higher vertical mixing and lower eddy thickness diffusivity, ocean heat and carbon uptake increase, resulting in a lower temperature change and higher cumulative emissions (see Figs. 1c,d). As the TCRE is defined as temperature change per cumulative emissions, TCRE values decrease for these mixing changes (Fig. 3b). Lower vertical mixing leads to higher TCRE values because the effects of changes in vertical mixing are symmetric. Increased isopycnal diffusivity leads to a marginally lower increase in heat flux and a slightly stronger increase in ocean carbon flux. This leads to a marginally stronger warming and slightly larger cumulative emissions. In total the TCRE is lower, and thus the increase in cumulative emission dominates over the increase in warming (cf. black line to red line in Figs. 1 and 3a).

The total range of the TCRE for all model versions at the time of CO_2 doubling is 1.2°–2.1°C EgC^{-1}. Changes in the vertical mixing parameters (green, blue, and purple curves in Fig. 3a) have a much stronger effect on the TCRE than changes in isopycnal mixing, even

though relative changes in the mixing along isopycnals are 300% (relative to the default value of A_h) and 200% for vertical mixing (relative to the center value of $k_{v,\text{const}}$). A stronger effect on ocean variables from changes in vertical mixing than from changes in isopycnal mixing are plausible as changes in vertical mixing have a strong effect on the density structure of the ocean.

This range in the TCRE is similar to the range in TCRE for CMIP5 models of 0.8°–2.4°C EgC^{-1} (Gillett et al. 2013) and the most likely range of 0.8°–2.5°C EgC^{-1} given in the Fifth Assessment Report of the IPCC (Collins et al. 2013). However, this should not imply that the TCRE spread between CMIP5 models is solely caused by variations in ocean mixing parameterization as a number of aspects, specifically in biogeochemical processes and the climate feedback parameter, are involved in the CMIP5 model TCRE range (MacDougall et al. 2016).

Plotting the temperature change at the time of doubling CO_2, a measure also referred to as TCR, versus the airborne fraction of cumulative CO_2 emissions (AF) at the time of CO_2 doubling, gives insights into the contribution of changes in the physical and the biogeochemical parts of the climate system toward the changes in the TCRE (Fig. 3b). The TCR is a measure of the physical response of the climate system to rising CO_2 levels and is affected by the effect of ocean heat flux on temperature and physical climate feedbacks. The AF is affected by both marine and terrestrial biogeochemical processes and thus is a measure of the biogeochemical response of the climate system. The boxes in Fig. 3b representing AF and TCR for each model version are nested. This means that changes in the TCR and in the AF (i.e., variations in physical and biogeochemical processes between model versions) affect variations in TCRE in the same direction. The exceptions are changes in the mixing along isopycnals, as under this mixing setting changes in the TCR are smaller and opposite in sign compared to changes in the AF. This goes along with minimal changes in the ocean heat uptake and slightly stronger changes in ocean carbon uptake (see Figs. 1a,b, red curve) for increased diffusivity along isopycnals.

The ocean heat uptake efficiency, defined as the ratio of net heat flux into the climate system to change in global mean surface air temperature, is another factor affected by ocean mixing. A decrease in ocean heat uptake efficiency means an increase in the TCR (Kuhlbrodt and Gregory 2012) and thus the TCRE. The ocean heat uptake efficiency increases for higher vertical mixing and for lower eddy thickness diffusivity (Fig. 3c), which corresponds to a decreased TCR and TCRE (Figs. 3a,b). Kuhlbrodt and Gregory (2012) link high ocean heat uptake efficiency to a less stratified ocean as more heat can be transported into the deeper ocean. This link holds true for both increased vertical mixing and decreased eddy thickness diffusivity. Decreased eddy thickness diffusivity leads to steeper isopycnal layers, especially in the Southern Ocean, and thus a weak stratification. The efficiency range given by Kuhlbrodt and Gregory (2012) is 0.27–0.83 $\text{W m}^{-2}\,^{\circ}\text{C}^{-1}$, which is calculated as ordinary least squares regression between net heat flux into the climate system and global mean surface air temperature change over the first 70 yr of a 1% CO_2 increase simulation. We find a range of 0.54–1.17 $\text{W m}^{-2}\,^{\circ}\text{C}^{-1}$ for an efficiency calculated the same way as for the CMIP5 models, with a value of 0.82 $\text{W m}^{-2}\,^{\circ}\text{C}^{-1}$ for the default mixing setting (Fig. 3c).

c. *Evolution of the TCRE over time*

Even with strong changes in ocean mixing parameters, the relationship between global mean temperature change and cumulative emissions remains close to linear within each mixing setting (Fig. 3a). However, when looking at how the TCRE evolves over time, the TCRE is not constant while atmospheric CO_2 increases (up to 20% divergence from time-mean TCRE value) in our model, but it is approximately constant (maximum 5% divergence from time-mean TCRE value) while atmospheric CO_2 is constant (Fig. 4a). Our finding of a nonconstant TCRE under increasing CO_2 concentration differs from the finding by Matthews et al. (2009) despite using the same model and prescribing a 1% atmospheric CO_2 increase because we apply a tighter definition of constancy and increase the time scale of our simulations beyond 70 yr. Considering a longer time scale emphasizes variation when the TCRE is plotted over time [cf. Fig. 4a in this study and Fig. 2a in Matthews et al. (2009)]. To further investigate which parts of the climate system contribute to the constancy of the TCRE over time or lead to divergence from a constant value, we consider the separation of the TCRE into the three terms given in Eq. (1). The first term in Eq. (1), the cumulative AF $\Delta C_A/\text{CE}$, is determined by the response of the ocean and land carbon sinks. The second term in Eq. (1) is the radiative forcing per unit change in atmospheric carbon $\text{RF}/\Delta C_A$, which expresses the radiative properties of CO_2. This term, referred to as radiative sensitivity from here on, follows a logarithmic relationship as the radiative forcing depends logarithmically on atmospheric CO_2 levels. The third term in Eq. (1) is the temperature sensitivity $\Delta T/\text{RF}$ (i.e., the amount of warming per unit radiative forcing). This sensitivity depends on climate feedbacks and ocean heat uptake and can be analytically described by the last two terms in Eq. (4).

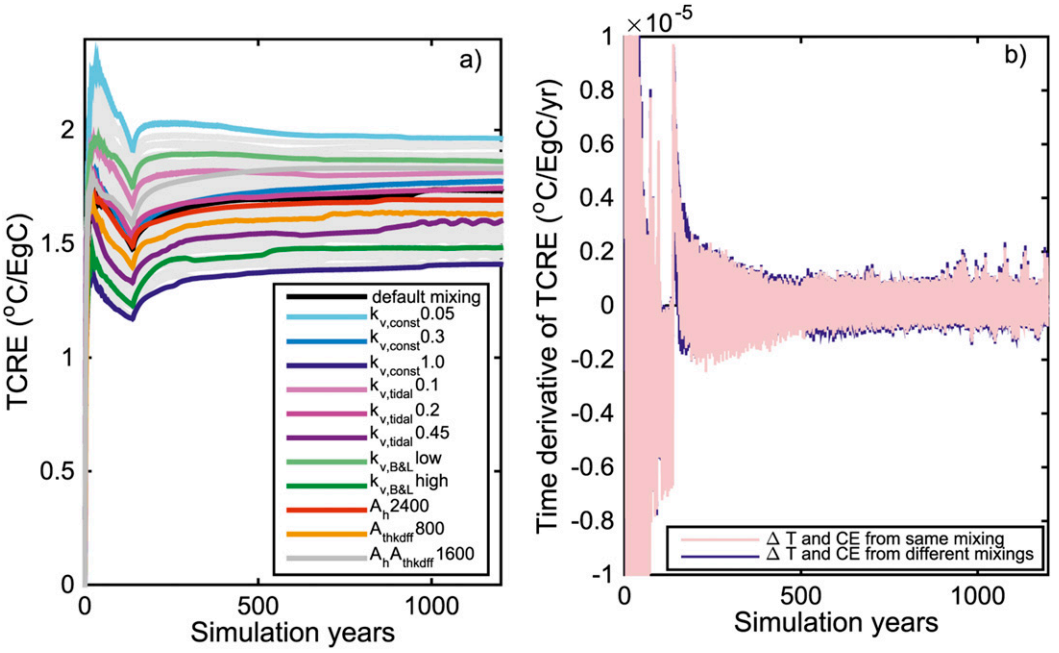

FIG. 4. (a) TCRE over time for different model versions. TCRE over time, with temperature change and cumulative emissions taken from model versions with different ocean mixing settings, is shown in light gray in the background. (b) Time derivatives of the TCRE with cumulative CO_2 emissions (CE) and global mean temperature change ΔT from the same model version (all model versions are shown in pink) and with CE and ΔT from different model versions (all combinations are shown in blue).

Equation (1) is applied to the simulation results in order to investigate the time dependency of AF, radiative sensitivity, and temperature sensitivity, as well as their role in the constancy of the TCRE. The discussion of the temporal evolution of AF, radiative sensitivity, temperature sensitivity, and the TCRE is separated in 1) the time period of increasing atmospheric CO_2 concentration (simulation years 0–139) and 2) the time period of constant atmospheric CO_2 concentration (simulation years 140–1200), when the system equilibrates to a new state and CO_2 emissions are very low.

1) INCREASING ATMOSPHERIC CO_2 CONCENTRATION

For all mixing settings the AF reaches a minimum and then increases again (Fig. 5a). It almost instantly reaches a value of around 0.7 and then declines to 0.5 at around year 40 and increases again to around 0.55–0.7. The AF can be expressed in terms of ocean and land uptake fraction [i.e., the fraction of cumulative CO_2 emissions absorbed by the land/ocean; see Eq. (2)]. The ocean carbon uptake fraction increases strongly at the beginning of the simulations and then declines slightly (Fig. 6a). In contrast, the land carbon uptake fraction first increases over time and then declines strongly (Fig. 6b) resulting from the saturation of land carbon sinks. The saturation of the land carbon sinks can be explained with climate–carbon cycle feedbacks, such as decreased net primary productivity in lower latitudes as a result of high temperatures or increased soil respiration under rising temperatures (Friedlingstein et al. 2006; Zickfeld et al. 2011). Thus, variations in the AF over time within each model version are mostly caused by the increase and decline of the land carbon uptake fraction. It should further be noted that the ocean carbon uptake fraction varies significantly between model versions, but the land carbon uptake fraction has only small variations between model versions. The land carbon uptake fraction does vary between model versions because the temperature differs, which has an effect on vegetation growth and soil respiration and in turn on land carbon uptake.

In contrast to the AF, radiative and temperature sensitivities decrease or increase monotonically. The radiative sensitivity declines over time (see Fig. 5b) as the rate of increase in radiative forcing declines with increasing CO_2 levels. The temperature sensitivity increases over time (see Fig. 5c). Using Eq. (3), this can be explained with a decrease of heat flux into the ocean per unit radiative forcing. Thus over the time of increasing atmospheric CO_2, AF, radiative sensitivity, and temperature sensitivity vary. The variations in these three terms do not compensate each other very well, resulting in the TCRE increasing first for one or two decades and then decreasing over time (see Fig. 4a). While the TCRE increases, the

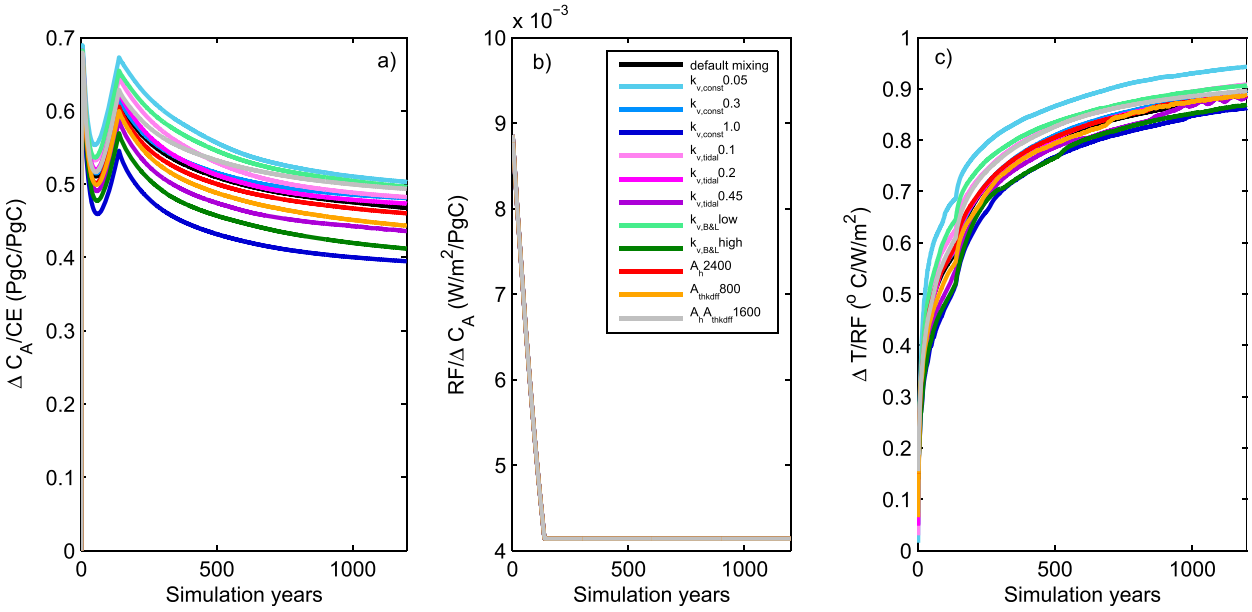

FIG. 5. Variation of the terms of the TCRE over time: (a) ΔC_A/CE (cumulative AF), (b) RF/ΔC_A (radiative sensitivity), and (c) ΔT/RF (temperature sensitivity), where ΔC_A is the change in atmospheric carbon burden, CE are the cumulative CO_2 emissions, RF is the radiative forcing, and ΔT is the global mean temperature change.

increase in temperature sensitivity dominates, as the other two terms of the TCRE decline over that time frame. As the TCRE starts declining, the decline in radiative sensitivity becomes dominant.

As all three terms of the TCRE vary, it could still be that the terms affected by ocean heat and carbon uptake cancel each other out. However, this is not the case (Fig. 7). The decline in heat flux per radiative forcing dominates over the increase in ocean carbon uptake fraction or land and ocean carbon uptake fraction added together (Fig. 7a, showing the terms containing ocean heat flux per radiative forcing and carbon uptake fractions, which are opposite in sign to ocean heat flux per radiative forcing and carbon uptake fractions). Therefore,

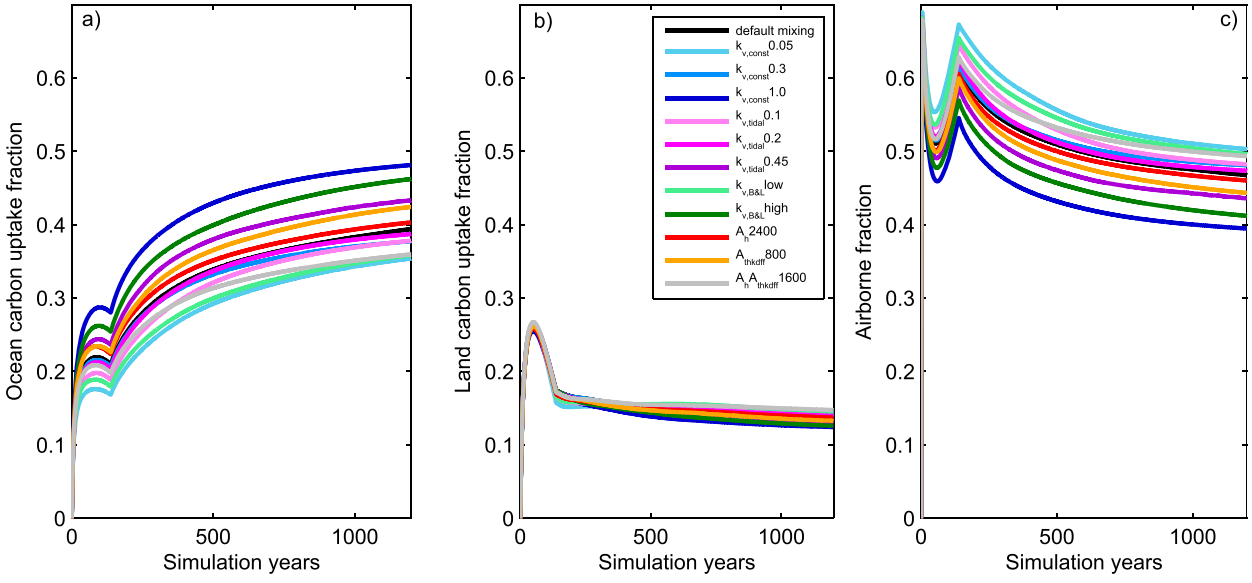

FIG. 6. (a) Ocean carbon uptake fraction ΔC_O/CE, (b) land carbon uptake fraction ΔC_L/CE, and (c) cumulative AF ΔC_A/CE over time. The terms ΔC_A, ΔC_O, and ΔC_L are the changes in atmospheric, ocean, and land carbon, respectively, and CE are the cumulative CO_2 emissions.

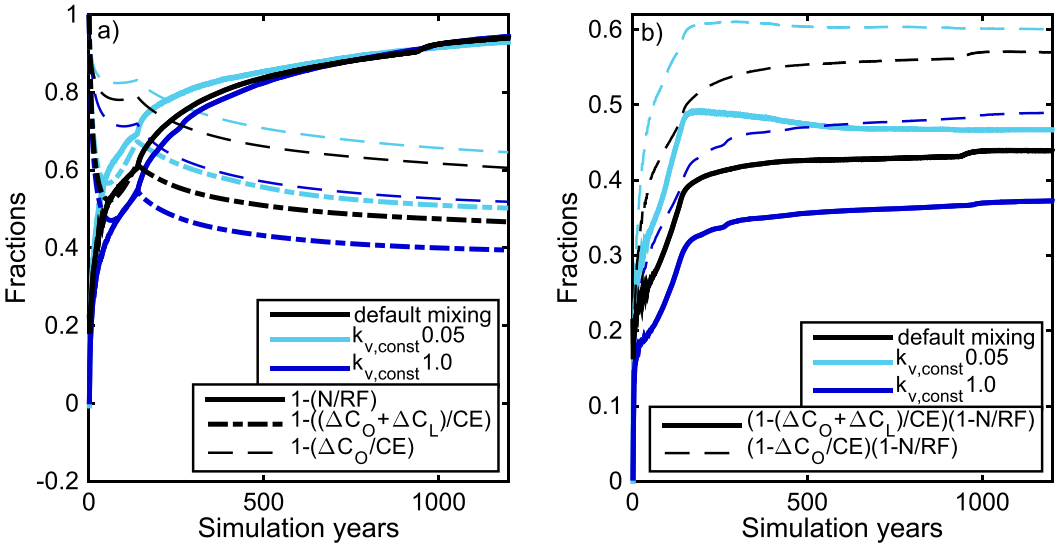

FIG. 7. Terms in the equations for TCRE [Eq. (4)] affected by ocean heat and carbon fluxes. (a) One minus the ratio of net heat flux into the climate system N (note that it differs from the ocean heat flux shown in Fig. 1, which is averaged over the surface area of the ocean rather than the entire Earth surface) and RF; one minus ΔC_O/CE, the ocean carbon uptake fraction, or $(\Delta C_O + \Delta C_L)$/CE, the combined carbon uptake fraction for land and ocean. (b) Terms in the equations for the TCRE containing ocean heat flux and ocean carbon flux, the latter one indirectly via ΔC_O.

both terms of the TCRE containing ocean heat and carbon flux together (i.e., multiplied with each other) increase while atmospheric CO_2 increases (Fig. 7b), and the effects of ocean heat and carbon uptake on the TCRE do not compensate each other.

The result that all three responses in the TCRE vary is consistent with the findings by MacDougall and Friedlingstein (2015) for exponentially increasing emission rates (the simulations presented here also have increasing emission rates).

2) CONSTANT ATMOSPHERIC CO_2 CONCENTRATION

While atmospheric CO_2 levels are constant (years 140–1200) the radiative sensitivity is constant, the cumulative AF declines, and the temperature sensitivity increases (see Fig. 5). The cumulative AF changes mostly because of an increase in the ocean uptake fraction; the land uptake fraction exhibits only minimal variations over time while atmospheric CO_2 levels are constant (see Fig. 6). The TCRE abruptly increases at year 140 (see Fig. 4a) because the emission rates change abruptly from increasing emission rates of up to 30 PgC yr^{-1} to close to zero emissions. After an adjustment time of about a decade the TCRE is approximately constant (see Fig. 4a) due to a compensation between the decline in AF and the increase in temperature sensitivity. The AF only varies as a result of changes in ocean carbon uptake, and the temperature sensitivity changes only as a result of changes in the ocean heat flux [see Eq. (4)]. Ocean carbon uptake declines, which leads to a less strong increase in the ocean carbon uptake fraction and thus a decrease in the airborne fraction. The decrease in ocean heat uptake leads to a stronger increase in temperature change and thus an increase in the temperature sensitivity. Hence the effects of ocean heat and carbon uptake have opposite effects on the TCRE. This suggests that the approximate constancy of the TCRE is caused by the compensation of the terms of the TCRE including ocean heat and carbon fluxes [see Eq. (4) and Fig. 7]. This compensation is independent of whether land carbon uptake is taken into account because the land uptake fraction does not change over time. The constancy of the land uptake fraction, however, may be model dependent. These results agree with the findings by Goodwin et al. (2015) and confirm the hypothesis that the compensating effects of ocean heat and carbon flux on the climate system lead to an approximately constant TCRE over time.

That ocean heat and carbon uptakes compensate each other despite the differences between them indicates that those differences (listed in the introduction in detail and summarized below) have secondary effects under constant atmospheric CO_2 concentrations. The time scales of air–sea equilibration are nine months for carbon but less than a month for heat. Both equilibration time scales are short compared to the decadal to centennial time scales considered in this study. The effects of ocean biology and solubility on ocean carbon uptake are difficult to diagnose, but these effects appear to be

relatively small while atmospheric CO_2 is constant. The effect of changes in ocean circulation on redistribution of heat and carbon and in turn on their air–sea fluxes together with the differences in the atmospheric boundary conditions could be small under constant forcing. However, this effect could play a role under increasing atmospheric CO_2 concentration where the effects of ocean heat and carbon uptake do not cancel each other out. It should be noted, though, that the effect of changes in ocean circulation on ocean heat uptake may be smaller in the UVic ESCM than in atmosphere–ocean general circulation models (AOGCMs) as changes in cloud cover increase the cooling effect from changes in ocean heat uptake resulting from changes in ocean circulation (Trossman et al. 2016), and the UVic ESCM does not include changes in clouds. Thus it could be that in AOGCMs the TCRE is not constant under constant forcing, at least while there is still an effect from changes in ocean circulation, as these changes in ocean circulation have a stronger effect on the ocean heat uptake than ocean carbon uptake and their effects on temperature (Winton et al. 2013). For example, Frölicher and Paynter (2015) show a nonconstant TCRE for the Earth system model (ESM) from GFDL from direct simulations and for other CMIP5 AOGCMs by temporally extending CMIP5 simulations using a theoretical approach.

The paragraphs above discuss to what extent and why the TCRE remains approximately constant over time within each mixing setting. Temporal variations in the TCRE, along with the compensating mechanism leading to an approximately constant TCRE over time while atmospheric CO_2 is constant, remain surprisingly consistent across model versions (see Figs. 4a and 5). To further test whether variations in mixing parameters cause compensating variations in ocean heat and carbon fluxes such that the TCRE remains constant, the TCRE is calculated using global mean temperature change from one model version and cumulative emissions from a different model version. We sampled over all possible combinations of temperature change and cumulative emissions (see Fig. 4a, gray shading) in such a way that for each ratio between temperature change and cumulative emissions, heat and carbon fluxes are affected by different ocean mixing settings. We find that the temporal evolution of the TCRE does not change significantly (see Figs. 4a,b, gray shading) despite temperature change being affected by, for example, low ocean heat flux and cumulative emissions being affected by high ocean carbon flux or vice versa. The time derivative of the TCRE (see Fig. 4b) is used as a measure of the constancy of the TCRE over time. This derivative is largely insensitive to whether temperature change and cumulative emissions are taken from the same or different model versions because the rate of change of the AF and the temperature sensitivity over time are similar enough between mixing settings (curves in Figs. 5a,c are approximate multiples of each other). These similarities in the temporal evolution of the AF and the temperature sensitivity between model versions with different mixing settings suggest that changes in ocean heat and carbon fluxes scale linearly with changes in vertical diffusivity (which have the largest effect on ocean heat and carbon fluxes). We show a linear correlation between ocean heat and carbon uptake and vertical diffusivity within each vertical mixing scheme (Fig. 2). This leads to higher (lower) ocean heat and carbon uptake and lower (higher) global mean temperature change and higher (lower) cumulative emissions but does not affect the trajectories of these variables. Therefore, the magnitude of the TCRE is affected if temperature change and cumulative emissions are taken from different simulations but the TCRE remains approximately constant over time. This linear scaling between diffusivities and ocean heat and carbon fluxes might be specific to the UVic ESCM as mixing parameterization and effects on the fluxes may vary.

4. Conclusions

Different model versions of the University of Victoria Earth System Climate Model are generated by changing the ocean mixing parameterization. These model versions are forced with a $1\%\,yr^{-1}$ increase in atmospheric CO_2 until quadrupling of the preindustrial CO_2 concentration and constant concentration thereafter. Despite significant changes in ocean mixing between model versions, the relationship between temperature change and cumulative emissions remains close to linear within each model version (see Fig. 3a). However, the magnitude of the TCRE differs between model versions with a total range of the TCRE at the time of CO_2 doubling of $1.2°–2.1°C\,EgC^{-1}$. These differences in the TCRE are due to changes in both the physical and biogeochemical response of the system as the two components of the TCRE, the AF at the time of CO_2 doubling and the TCR, change in the same direction in each model version (i.e., a larger AF is associated with a larger TCR and vice versa; see Fig. 3b). Variations in the vertical ocean mixing lead to stronger changes in heat and carbon fluxes, and thus in the TCRE, than changes in mixing along isopycnals (see Figs. 1a,b). Therefore, constraining the vertical ocean mixing parameterization could help constrain the TCRE. Thus, a next step could be to run a historical

simulations with the different model versions in order to compare them to observational data such as surface air temperature data or ocean tracer distributions.

The TCRE is approximately constant while atmospheric CO_2 concentrations are constant (5% variation from mean TCRE value), but it is not constant (up to 20% deviation from mean TCRE value) while atmospheric CO_2 increases (see Fig. 4a). Separating the TCRE into AF, radiative sensitivity (radiative forcing per unit change in atmospheric CO_2), and temperature sensitivity (temperature change per unit radiative forcing) reveals that all three sensitivities vary while atmospheric CO_2 concentrations increase, but changes in temperature sensitivity and AF compensate each other in all model versions while atmospheric CO_2 concentrations are held constant (see Fig. 5). This compensation is due to the compensating effects of ocean heat and carbon fluxes on the TCRE. The TCRE remains approximately constant even if the temperature sensitivity and AF, which are determined by ocean heat and carbon fluxes respectively, are taken from model versions with different ocean mixing settings. This could be explained with temperature sensitivity and AF having similar trajectories under different mixing settings. This suggests that changes in ocean heat and carbon fluxes scale linearly with changes in vertical mixing (see Fig. 2). The effects of changes in mixing along isopycnals on ocean heat and carbon fluxes, and in turn on temperature sensitivity and AF, are too small to affect the temporal constancy of the TCRE.

In summary, the responses of ocean heat and carbon fluxes do not compensate each other very well, and the TCRE is not constant while atmospheric CO_2 concentrations increase, or more generally while emission rates vary strongly, but is approximately constant while atmospheric CO_2 is constant. This constancy of the TCRE arises because of the compensating effects of ocean heat and carbon fluxes. The land carbon uptake plays only a minor role while atmospheric CO_2 concentrations are constant as the land carbon uptake fraction exhibits only small variations. Thus for the case of constant atmospheric CO_2 our findings confirm the hypothesis that the evolution of ocean heat and carbon fluxes over time is similarly determined by vertical mixing processes, leading to compensating changes in temperature sensitivity and AF, and an approximately constant TCRE.

Acknowledgments. K. Zickfeld and D. Ehlert acknowledge support from the Natural Sciences and Engineering Research Council of Canada (NSERC) Discovery Grant Program (402402/2011). This research was enabled in part by computing resources provided by Westgrid and Compute Canada.

REFERENCES

Allen, M. R., D. J. Frame, C. Huntingford, C. D. Jones, J. A. Lowe, M. Meinshausen, and N. Meinshausen, 2009: Warming caused by cumulative carbon emissions towards the trillionth tonne. *Nature*, **458**, 1163–1166, doi:10.1038/nature08019.

Archer, D., 1996: A data-driven model of the global calcite lysocline. *Global Biogeochem. Cycles*, **10**, 511–526, doi:10.1029/96GB01521.

Bindoff, N., and Coauthors, 2013: Detection and attribution of climate change: From global to regional. *Climate Change 2013: The Physical Science Basis*, T. F. Stocker et al., Eds., Cambridge University Press, 867–952, doi:10.1017/CBO9781107415324.022.

Collins, M., and Coauthors, 2013: Long-term climate change: Projections, commitments and irreversibility. *Climate Change 2013: The Physical Science Basis*, T. F. Stocker et al., Eds., Cambridge University Press, 1029–1136, doi:10.1017/CBO9781107415324.024.

Cox, P. M., 2001: Description of the TRIFFID dynamic global vegetation model. Met Office Hadley Centre Tech. Note 24, 17 pp.

——, R. A. Betts, C. B. Bunton, R. L. H. Essery, P. R. Rowntree, and J. Smith, 1999: The impact of new land surface physics on the GCM simulation of climate and climate sensitivity. *Climate Dyn.*, **15**, 183–203, doi:10.1007/s003820050276.

Eby, M., K. Zickfeld, A. Montenegro, D. Archer, K. J. Meissner, and A. J. Weaver, 2009: Lifetime of anthropogenic climate change: Millennial time scales of potential CO_2 and surface temperature perturbations. *J. Climate*, **22**, 2501–2511, doi:10.1175/2008JCLI2554.1.

Ewen, T. L., A. J. Weaver, and M. Eby, 2004: Sensitivity of the inorganic ocean carbon cycle to future climate warming in the UVic coupled model. *Atmos.–Ocean*, **42**, 23–42, doi:10.3137/ao.420103.

Friedlingstein, P., and Coauthors, 2006: Climate–carbon cycle feedback analysis: Results from the C4MIP model intercomparison. *J. Climate*, **19**, 3337–3353, doi:10.1175/JCLI3800.1.

Frölicher, T. L., and D. J. Paynter, 2015: Extending the relationship between global warming and cumulative carbon emissions to multi-millennial timescales. *Environ. Res. Lett.*, **10**, 075002, doi:10.1088/1748-9326/10/7/075002.

——, J. L. Sarmiento, D. J. Paynter, J. P. Dunne, J. P. Krasting, and M. Winton, 2015: Dominance of the Southern Ocean in anthropogenic carbon and heat uptake in CMIP5 models. *J. Climate*, **28**, 862–886, doi:10.1175/JCLI-D-14-00117.1.

Gent, P. R., and J. C. McWilliams, 1990: Isopycnal mixing in ocean circulation models. *J. Phys. Oceanogr.*, **20**, 150–155, doi:10.1175/1520-0485(1990)020<0150:IMIOCM>2.0.CO;2.

Gillett, N. P., V. K. Arora, D. Matthews, and M. R. Allen, 2013: Constraining the ratio of global warming to cumulative CO_2 emissions using CMIP5 simulations. *J. Climate*, **26**, 6844–6858, doi:10.1175/JCLI-D-12-00476.1.

Gnanadesikan, A., 1999: A simple predictive model for the structure of the oceanic pycnocline. *Science*, **283**, 2077–2079, doi:10.1126/science.283.5410.2077.

——, R. Abernathey, and M.-A. Pradal, 2015a: Exploring the isopycnal mixing and helium-heat paradoxes in a suite of Earth system models. *Ocean Sci.*, **11**, 591–605, doi:10.5194/os-11-591-2015.

——, M.-A. Pradal, and R. Abernathey, 2015b: Isopycnal mixing by mesoscale eddies significantly impacts oceanic anthropogenic carbon uptake. *Geophys. Res. Lett.*, **42**, 4249–4255, doi:10.1002/2015GL064100.

Goes, M., N. M. Urban, R. Tonkonojenkov, M. Haran, A. Schmittner, and K. Keller, 2010: What is the skill of ocean tracers in reducing uncertainties about ocean diapycnal mixing and projections of the Atlantic meridional overturning circulation? *J. Geophys. Res.*, **115**, C12006, doi:10.1029/2010JC006407.

Goodwin, P., R. G. Williams, and A. Ridgwell, 2015: Sensitivity of climate to cumulative carbon emissions due to compensation of ocean heat and carbon uptake. *Nat. Geosci.*, **8**, 29–34, doi:10.1038/ngeo2304.

Gregory, J. M., T. Andrews, and P. Good, 2015: The inconstancy of the transient climate response parameter under increasing CO_2. *Philos. Trans. Roy. Soc. London*, **373A**, 20140417, doi:10.1098/rsta.2014.0417.

Herrington, T., and K. Zickfeld, 2014: Path independence of climate and carbon cycle response over a broad range of cumulative carbon emissions. *Earth Syst. Dyn.*, **5**, 409–422, doi:10.5194/esd-5-409-2014.

Krasting, J. P., J. P. Dunne, E. Shevliakova, and R. J. Stouffer, 2014: Trajectory sensitivity of the transient climate response to cumulative carbon emissions. *Geophys. Res. Lett.*, **41**, 2520–2527, doi:10.1002/2013GL059141.

Kuhlbrodt, T., and J. M. Gregory, 2012: Ocean heat uptake and its consequences for the magnitude of sea level rise and climate change. *Geophys. Res. Lett.*, **39**, L18608, doi:10.1029/2012GL052952.

Leduc, M., H. D. Matthews, and R. de Elía, 2015: Quantifying the limits of a linear temperature response to cumulative CO_2 emissions. *J. Climate*, **28**, 9955–9968, doi:10.1175/JCLI-D-14-00500.1.

MacDougall, A. H., and P. Friedlingstein, 2015: The origin and limits of the near proportionality between climate warming and cumulative CO_2 emissions. *J. Climate*, **28**, 4217–4230, doi:10.1175/JCLI-D-14-00036.1.

——, N. C. Swart, and R. Knutti, 2016: The uncertainty in the transient climate response to cumulative CO_2 emissions arising from the uncertainty in physical climate parameters. *J. Climate*, **30**, 813–827, doi:10.1175/JCLI-D-16-0205.1.

Matthews, H. D., N. P. Gillett, P. A. Stott, and K. Zickfeld, 2009: The proportionality of global warming to cumulative carbon emissions. *Nature*, **459**, 829–832, doi:10.1038/nature08047.

Meissner, K. J., J. Weaver, H. D. Matthews, and P. M. Cox, 2003: The role of land surface dynamics in glacial inception: A study with the UVic Earth System Model. *Climate Dyn.*, **21**, 515–537, doi:10.1007/s00382-003-0352-2.

Olson, R., R. Sriver, M. Goes, N. M. Urban, H. D. Matthews, M. Haran, and K. Keller, 2012: A climate sensitivity estimate using Bayesian fusion of instrumental observations and an Earth system model. *J. Geophys. Res.*, **117**, D04103, doi:10.1029/2011JD016620.

Raupach, M. R., and Coauthors, 2014: Sharing a quota on cumulative carbon emissions. *Nat. Climate Change*, **4**, 873–879, doi:10.1038/nclimate2384.

Ross, A., H. D. Matthews, A. Schmittner, and Z. Kothavala, 2012: Assessing the effects of ocean diffusivity and climate sensitivity on the rate of global climate change. *Tellus*, **64B**, 17733, doi:10.3402/tellusb.v64i0.17733.

Schmittner, A., and A. J. Weaver, 2001: Dependence of multiple climate states on ocean mixing parameters. *Geophys. Res. Lett.*, **28**, 1027–1030, doi:10.1029/2000GL012410.

——, A. Oschlies, X. Giraud, M. Eby, and H. L. Simmons, 2005: A global model of the marine ecosystem for long-term simulations: Sensitivity to ocean mixing, buoyancy forcing, particle sinking, and dissolved organic matter cycling. *Global Biogeochem. Cycles*, **19**, GB3004, doi:10.1029/2004GB002283.

——, N. M. Urban, K. Keller, and D. Matthews, 2009: Using tracer observations to reduce the uncertainty of ocean diapycnal mixing and climate-carbon cycle projections. *Global Biogeochem. Cycles*, **23**, GB4009, doi:10.1029/2008GB003421.

Solomon, S., G.-K. Plattner, R. Knutti, and P. Friedlingstein, 2009: Irreversible climate change due to carbon dioxide emissions. *Proc. Natl. Acad. Sci. USA*, **106**, 1704–1709, doi:10.1073/pnas.0812721106.

Tokarska, K. B., N. P. Gillett, A. J. Weaver, V. K. Arora, and M. Eby, 2016: The climate response to five trillion tonnes of carbon. *Nat. Climate Change*, **6**, 851–855, doi:10.1038/nclimate3036.

Trossman, D. S., J. B. Palter, T. M. Merlis, Y. Huang, and Y. Xia, 2016: Large-scale ocean circulation-cloud interactions reduce the pace of transient climate change. *Geophys. Res. Lett.*, **43**, 3935–3943, doi:10.1002/2016GL067931.

Weaver, A. J., and Coauthors, 2001: The UVic Earth System Climate Model: Model description, climatology, and applications to past, present and future climates. *Atmos.–Ocean*, **39**, 361–428, doi:10.1080/07055900.2001.9649686.

Williams, R. G., P. Goodwin, V. M. Rouusenov, and L. Bopp, 2016: A framework to understand the transient climate response to emissions. *Environ. Res. Lett.*, **11**, 15003, doi:10.1088/1748-9326/11/1/015003.

Winton, M., S. M. Griffies, B. L. Samuels, J. L. Sarmiento, and T. L. Frölicher, 2013: Connecting changing ocean circulation with changing climate. *J. Climate*, **26**, 2268–2278, doi:10.1175/JCLI-D-12-00296.1.

Zickfeld, K., M. Eby, H. D. Matthews, and A. J. Weaver, 2009: Setting cumulative emissions targets to reduce the risk of dangerous climate change. *Proc. Natl. Acad. Sci. USA*, **106**, 16 129–16 134, doi:10.1073/pnas.0805800106.

——, ——, ——, A. Schmittner, and A. J. Weaver, 2011: Nonlinearity of carbon cycle feedbacks. *J. Climate*, **24**, 4255–4275, doi:10.1175/2011JCLI3898.1.

——, A. H. MacDougall, and H. D. Matthews, 2016: On the proportionality between global temperature change and cumulative CO_2 emissions during periods of net negative CO_2 emissions. *Environ. Res. Lett.*, **11**, 055006, doi:10.1088/1748-9326/11/5/055006.